J|A|C|S ARTICLES

Published on Web 01/19/2010

Hydrogenation: A Simple Approach To Realize Semiconductor−Half-Metal−Metal Transition in Boron Nitride Nanoribbons

Wei Chen,[†] Yafei Li,[‡] Guangtao Yu,[§] Chen-Zhong Li,[||] Shengbai B. Zhang,[⊥] Zhen Zhou,*[,‡] and Zhongfang Chen*[,†]

Department of Chemistry, Institute for Functional Nanomaterials, University of Puerto Rico, San Juan, Puerto Rico 00931, Institute of New Energy Material Chemistry, Nankai University, Tianjin 300071, People's Republic of China, The State Key Laboratory of Theoretical and Computational Chemistry, Institute of Theoretical Chemistry, Jilin University, Changchun 130023, People's Republic of China, Biomedical Engineering Department, Florida International University, Miami, Florida 33174, and Department of Physics, Applied Physics, and Astronomy, Rensselaer Polytechnic Institute, Troy, New York 12180

Received October 5, 2009; E-mail: zhouzhen@nankai.edu.cn; zhongfangchen@gmail.com

Abstract: The intriguing electronic and magnetic properties of fully and partially hydrogenated boron nitride nanoribbons (BNNRs) were investigated by means of first-principles computations. Independent of ribbon width, fully hydrogenated armchair BNNRs are nonmagnetic semiconductors, while the zigzag counterparts are magnetic and metallic. The partially hydrogenated zigzag BNNRs (using hydrogenated BNNRs and pristine BNNRs as building units) exhibit diverse electronic and magnetic properties: they are nonmagnetic semiconductors when the percentage of hydrogenated BNNR blocks is minor, while a semiconductor→half-metal→metal transition occurs, accompanied by a nonmagnetic→magnetic transfer, when the hydrogenated part is dominant. Although the half-metallic property is not robust when the hydrogenation ratio is large, this behavior is sustained for partially hydrogenated zigzag BNNRs with a smaller degree of hydrogenation. Thus, controlling the hydrogenation ratio can precisely modulate the electronic and magnetic properties of zigzag BNNRs, which endows BN nanomaterials many potential applications in the novel integrated functional nanodevices.

1. Introduction

Graphene, a two-dimensional (2D) sheet of sp^2-hybridized carbon, is taking us into the new material revolution,[1−3] because the long-range π-conjugation makes it exhibit extraordinary thermal, mechanical, and electrical properties.[4−9] For example, graphene is the strongest material ever measured,[4] and its ability to conduct electricity is the best among the known materials at room temperature.[6] Stimulated by these outstanding properties, graphene-based materials[10−36] attracted extensive experimental and theoretical investigations.

By carving the 2D graphene, one-dimensional (1D) graphene nanoribbons (GNRs) have been realized.[1] Because of the change of dimensionality, GNRs display unusual electronic and magnetic properties different from graphene.[12−29] Both first-principles computations[17,22,23] and experimental investigations[25,26] revealed a nonzero band gap for GNRs independent of their width and chirality. Zigzag GNRs are magnetic,[20,22] while armchair GNRs are nonmagnetic. Moreover, theoretical studies predict that either electric field[27] or chemical functionalization[28−30] can make GNRs half metals, which have potential application in spintronics.

Furthermore, by hydrogenating graphene, 2D graphane (fully hydrogenated graphene) was obtained experimentally[10,31] and can be considered as an electronic insulator.[10] A 2D graphane layer,[32] hydrogenation of graphene with defects,[33,34] and fluorine-substituted graphane[35] were theoretically studied in detail. Besides graphane, the electronic and magnetic properties of partially hydrogenated graphene have also been investigated.[36−38] Moreover, 1D graphane nanoribbons can be experimentally realized by cutting the 2D graphane, similar to the case of GNRs, or by hydrogenating GNRs, like the formation process from graphene to graphane. Recent computational

[†] University of Puerto Rico.
[‡] Nankai University.
[§] Jilin University.
[||] Florida International University.
[⊥] Rensselaer Polytechnic Institute.

(1) Novoselov, K. S.; Geim, A. K.; Morozov, S. V.; Jiang, D.; Zhang, Y.; Dubonos, S. V.; Grigoreva, I. V.; Firsov, A. A. *Science* **2004**, *306*, 666–669.
(2) Novoselov, K. S.; Jiang, D.; Schedin, F.; Booth, T. J.; Khotkevich, V. V.; Morozov, S. V.; Geim, A. K. *Proc. Natl. Acad. Sci. U.S.A.* **2005**, *102*, 10451–10453.
(3) Allen, M. J.; Tung, V. C.; Kaner, R. B. *Chem. Rev.* DOI: 10.1021/cr900070d.
(4) Lee, G.; Wei, X.; Kysar, J. W.; Hone, J. *Science* **2008**, *321*, 385–388.
(5) Zhang, Y.; Tan, Y.-W.; Stormer, H. L.; Kim, P. *Nature* **2005**, *438*, 201–204.
(6) Ponomarenko, L. A.; Schedin, F.; Katsnelson, M. I.; Yang, R.; Hill, E. W.; Novoselov, K. S.; Geim, A. K. *Science* **2008**, *320*, 356–358.
(7) Kan, E. J.; Li, Z. Y.; Yang, J. L. *Nano* **2008**, *3*, 433–442.
(8) Berger, C.; Song, Z.; Li, X.; Wu, X.; Brown, N.; Naud, C.; Mayou, D.; Li, T.; Hass, J.; Marchenkov, A. N.; Conrad, E. H.; First, P. N.; Heer, W. A. d. *Science* **2006**, *312*, 1191–1196.
(9) Ci, L.; Xu, Z.; Wang, L.; Gao, W.; Ding, F.; Kelly, K.; Yakobson, B. I.; Ajayan, P. *Nano Res.* **2008**, *1*, 116–122.

studies show that 1D graphane nanoribbons have favorable formation energies and are wide-band gap semiconductors and nonmagnetic,[39] which is obviously different from the case of GNRs. Very recently, Xiang et al.'s computations revealed that the partially hydrogenated wide GNRs have similar electronic and magnetic properties to the narrow GNRs representing their graphene parts.[40]

Extensive studies on carbon nanosystems including GNRs and graphane nanoribbons have also stimulated researchers' great interest in inorganic nanotubes/nanoribbons, such as BN nanotubes,[41−45] and BNC,[46] B,[47] BC_3,[48] B_2C,[49] SiC,[50] ZnO,[51] MoS_2[52] nanoribbons, particularly BN nanoribbons (BNNRs),[53−61] a structural analogy of GNRs. In view of the large ionicity of BN, BNNRs exhibit some unique properties different from GNRs. Independent of their width and chirality, perfect BNNRs display semiconductor behaviors.[47] The bare zigzag BNNRs (zBNNRs)[53,60] and H-terminated BNNRs[54] are magnetic and nonmagnetic, respectively. However, two-hydrogen-terminated zBNNRs are magnetic and metallic.[59] The formation of Stone−Wales (SW) defects[62] and edge modification[58] with F, Cl, OH, and NO_2 groups can change the band gap of the BNNRs, although these decorated BNNRs still keep semiconducting character. An extra transversal electric field can control the band gap of bare zBNNRs to undergo metallic−semiconducting−half-metallic transition.[46] Moreover, the BNNRs with only B edge terminated by hydrogen present half-metallic characteristics.[60,61] These interesting electronic properties make BNNRs promising for many potential applications in nanoelectronics.

Great progress has been achieved in synthesizing BN nanosheets.[63−71] Zhi et al.[63] recently synthesized large-scale BN nanosheets and used them to improve thermal and mechanical properties of polymeric composites. Also, the single-layer and few-atom-layer hexagonal BN sheets have been experimentally realized[64−71] and are proposed as an alternative carbon graphene for plane electronics, where the lithography technique can be conveniently employed. Similar to the GNRs, it is possible to obtain BNNRs by cutting single-layer hexagonal BN sheets. Further hydrogenation process of BNNRs may lead to fully or partially hydrogenated BNNRs. Because the electronic and magnetic properties of GNRs are different from those of graphane nanoribbons, it is attractive to investigate the relevant properties of the fully and partially hydrogenated BNNRs. However, to our best knowledge, these hydrogenated BNNRs have not received any study so far.

(10) Elias, D. C.; Nair, R. R.; Mohiuddin, T. M. G.; Morozov, S. V.; Blake, P.; Halsall, M. P.; Ferrairi, A. C.; Boukhvalov, D. W.; Katsnelson, M. I.; Geim, A. K. *Science* **2009**, *323*, 610–613.
(11) Hod, O.; Scuseria, G. E. *Nano Lett.* **2009**, *9*, 2619–2622.
(12) Li, Y.; Zhou, Z.; Shen, P.; Chen, Z. *ACS Nano* **2009**, *3*, 1952–1958.
(13) Ezawa, M. *Phys. Rev. B* **2006**, *73*, 045432.
(14) Fujita, M.; Wakabayashi, K.; Nakada, K.; Kusakabe, K. *J. Phys. Soc. Jpn.* **1996**, *65*, 1920–1923.
(15) Wakabayashi, K.; Fujita, M.; Ajiki, H.; Sigrist, M. *Phys. Rev. B* **1999**, *59*, 8271–8282.
(16) Nakada, K.; Fujita, M.; Dresselhaus, G.; Dresselhaus, M. S. *Phys. Rev. B* **1996**, *54*, 17954–17961.
(17) Son, Y.; Cohen, M.; Louie, S. *Phys. Rev. Lett.* **2006**, *97*, 216803.
(18) Ezawa, M. *Physica E* **2008**, *40*, 1421–1423.
(19) Ezawa, M. *Phys. Rev. B* **2007**, *76*, 245415.
(20) Kudin, K. N. *ACS Nano* **2008**, *2*, 516–522.
(21) Wassman, T.; Seitsonen, A. P.; Saitta, A. M.; Lazzeri, M.; Mauri, F. *Phys. Rev. Lett.* **2008**, *101*, 096402.
(22) Barone, V.; Hod, O.; Scuseria, G. E. *Nano Lett.* **2006**, *6*, 2748–2754.
(23) Jiang, D. E.; Sumpter, B. G.; Dai, S. *J. Chem. Phys.* **2007**, *127*, 124703.
(24) Jiang, D. E.; Sumpter, B. G.; Dai, S. *J. Chem. Phys.* **2007**, *126*, 134701.
(25) Ritter, K. A.; Lyding, J. W. *Nat. Mater.* **2009**, *8*, 235–242.
(26) Li, X. L.; Wang, X. R.; Zhang, L.; Lee, S. W.; Dai, H. J. *Science* **2008**, *319*, 1229–1232.
(27) Son, Y. W.; Cohen, M. L.; Louie, S. G. *Nature (London)* **2006**, *444*, 347–349.
(28) Hod, O.; Barone, V.; Peralta, J. E.; Scuseria, G. E. *Nano Lett.* **2007**, *7*, 2295–2299.
(29) Kan, E. J.; Li, Z. Y.; Yang, J. L.; Hou, J. G. *J. Am. Chem. Soc.* **2008**, *130*, 4224–4225.
(30) Wu, M.; Wu, X.; Gao, Y.; Zeng, X. C. *Appl. Phys. Lett.* **2009**, *94*, 223111.
(31) Ryu, S. M.; Han, M. Y.; Maultzsch, J.; Heinz, T. F.; Kim, P.; Steigerwald, M. L.; Brus, L. E. *Nano Lett.* **2008**, *8*, 4597–4602.
(32) Sofo, J. O.; Chaudhari, A. S.; Barber, G. D. *Phys. Rev. B* **2007**, *75*, 153401.
(33) Boukhvalov, D. W.; Katsnelson, M. I. *Nano Lett.* **2008**, *8*, 4373–4379.
(34) Pujari, B. S.; Kanhere, D. G. *J. Phys. Chem. C* **2009**, *113*, 21063–21067.
(35) Lu, N.; Li, Z. Y.; Yang, J. L. *J. Phys. Chem. C* **2009**, *113*, 16741–16746.
(36) Zhou, J.; Wang, Q.; Sun, Q.; Chen, X. S.; Kawazoe, Y.; Jena, P. *Nano Lett.* **2009**, *9*, 3867–3870.
(37) Singh, A. K.; Yakobson, B. I. *Nano Lett.* **2009**, *9*, 1540–1543.
(38) Boukhvalov, D. W.; Katsnelson, M. I.; Lichtenstein, A. I. *Phys. Rev. B* **2008**, *77*, 035427.
(39) Li, Y.; Zhou, Z.; Shen, P.; Chen, Z. *J. Phys. Chem. C* **2009**, *113*, 15043–15045.
(40) Xiang, H. J.; Kan, E.; Wei, S. H.; Whangbo, M. H.; Yang, J. L. *Nano Lett.* **2009**, *9*, 4025–4030.
(41) Schmidt, T. M.; Baierle, R. J.; Piquini, P.; Fazzio, A. *Phys. Rev. B* **2003**, *67*, 113407.
(42) Wu, R. Q.; Liu, L.; Peng, G. W.; Feng, Y. P. *Appl. Phys. Lett.* **2005**, *86*, 122510.
(43) Si, M. S.; Xue, D. S. *Europhys. Lett.* **2006**, *76*, 664.
(44) Li, F.; Zhu, Z.; Yao, X.; Lu, G.; Zhao, M.; Xia, Y.; Chen, Y. *Appl. Phys. Lett.* **2008**, *92*, 102515.
(45) Zhang, Z.; Guo, W. *J. Am. Chem. Soc.* **2009**, *131*, 6874–6879.
(46) Nakamura, J.; Nitta, T.; Natori, A. *Phys. Rev. B* **2005**, *72*, 205429.
(47) Ding, Y.; Yang, X.; Ni, J. *Appl. Phys. Lett.* **2008**, *93*, 043107.
(48) Ding, Y.; Wang, Y. L.; Ni, J. *Appl. Phys. Lett.* **2009**, *94*, 073111.
(49) Wu, X.; Pei, Y.; Zeng, X. C. *Nano Lett.* **2009**, *9*, 1577–1582.
(50) Sun, L.; Li, Y.; Li, Z.; Li, Q.; Zhou, Z.; Chen, Z.; Yang, J.; Hou, J. G. *J. Chem. Phys.* **2008**, *129*, 174114.
(51) Botello-Méndez, A. R.; López-Urías, F.; Terrones, M.; Terrones, H. *Nano Lett.* **2008**, *8*, 1562–1565.
(52) Li, Y.; Zhou, Z.; Zhang, S.; Chen, Z. *J. Am. Chem. Soc.* **2008**, *130*, 16739–16744.
(53) Barone, V.; Peralta, J. E. *Nano Lett.* **2008**, *8*, 2210–2214.
(54) Du, A.; Smith, S. C.; Lu, G. *Chem. Phys. Lett.* **2007**, *447*, 181–186.
(55) Zhang, Z.; Guo, W. *Phys. Rev. B* **2008**, *77*, 075403.
(56) Park, C. H.; Louie, S. G. *Nano Lett.* **2008**, *8*, 2200–2203.
(57) Jin, C.; Lin, F.; Suenaga, K.; Iijima, S. *Phys. Rev. Lett.* **2009**, *102*, 195505.
(58) Wu, X.; Wu, M.; Zeng, X. C. *Front. Phys. China* **2009**, *4*, 367–372.
(59) Ding, Y.; Wang, Y. L.; Ni, J. *Appl. Phys. Lett.* **2009**, *94*, 233107.
(60) Lai, L.; Lu, J.; Wang, L.; Luo, G.; Zhou, J.; Qin, R.; Gao, Z.; Mei, W. N. *J. Phys. Chem. C* **2009**, *113*, 2273–2276.
(61) Zheng, F.; Zhou, G.; Liu, Z.; Wu, J.; Duan, W.; Gu, B.; Zhang, S. B. *Phys. Rev. B* **2008**, *78*, 205415.
(62) Chen, W.; Li, Y.; Yu, G. T.; Zhou, Z.; Chen, Z. *J. Chem. Theory Comput.* **2009**, *5*, 3088–3095.
(63) Zhi, C.; Bando, Y.; Tang, C.; Kuwahara, H.; Golberg, D. *Adv. Mater.* **2009**, *21*, 2889–2893.
(64) Nagashima, A.; Tejima, N.; Gamou, Y.; Kawai, T.; Oshima, C. *Phys. Rev. Lett.* **1995**, *75*, 3918–3921.
(65) Pacilé, D.; Meyer, J. C.; Girit, Ç. Ö.; Zettl, A. *Appl. Phys. Lett.* **2008**, *92*, 133107.
(66) Han, W.-Q.; Wu, L.; Zhu, Y.; Watanabe, K.; Taniguchi, T. *Appl. Phys. Lett.* **2008**, *93*, 223103.
(67) Meyer, J. C.; Chuvilin, A.; Algara-Siller, G.; Biskupek, J.; Kaiser, U. *Nano Lett.* **2009**, *9*, 2683–2689.
(68) Corso, M.; Greber, T.; Osterwalder, J. *Surf. Sci.* **2005**, *577*, L78–L84.
(69) Morscher, M.; Corso, M.; Greber, T.; Osterwalder, J. *Surf. Sci.* **2006**, *600*, 3280–3284.
(70) Goriachko, A.; He, Y. B.; Knapp, M.; Over, H.; Corso, M.; Brugger, T.; Berner, S.; Osterwalder, J.; Greber, T. *Langmuir* **2007**, *23*, 2928–2931.
(71) Lin, Y.; Williams, T. V.; Connell, J. W. *J. Phys. Chem. Lett.* **2010**, *1*, 277–283.

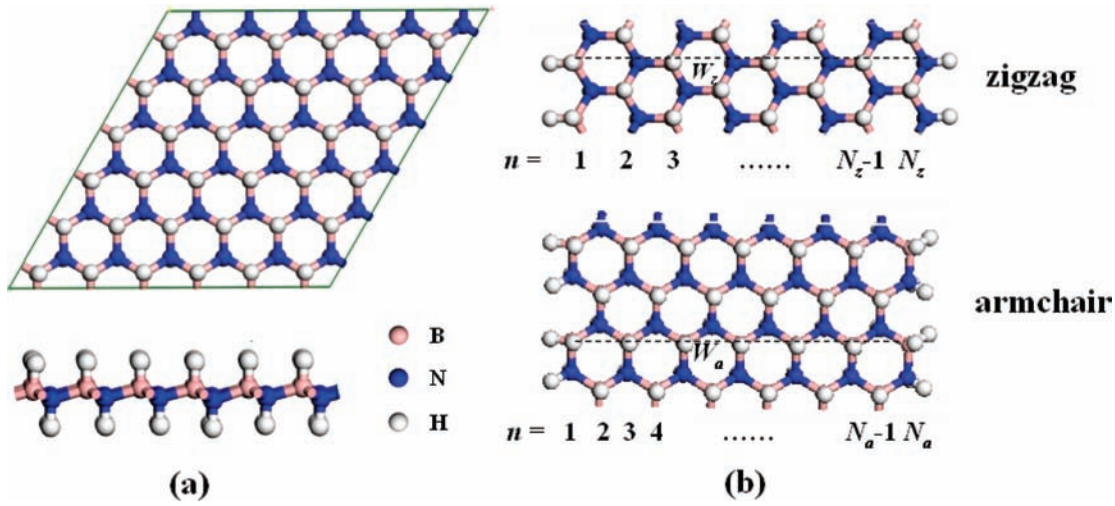

Figure 1. (a) Top and side views of the 2D fully hydrogenated BN single layer. (b) Geometric structures of fully hydrogenated zigzag and armchair BNNRs. The blue, pink, and white colors represent N, B, and H atoms, respectively.

In this work, we performed detailed first-principles computations to investigate the formation energies, electronic, and magnetic properties of the fully and partially hydrogenated BNNRs. The following questions are mainly addressed: (1) Are the fully and partially hydrogenated BNNRs nonmagnetic semiconductors similar to the analogous graphane nanoribbons or magnetic metals such as two-hydrogen-terminated zBNNRs? (2) Do the fully hydrogenated BNNRs have favorable formation energies, as graphane nanoribbons? (3) How will the ribbon width and chirality and hydrogen concentration affect the electronic and magnetic properties? The answers to these questions will gain us a deeper understanding of the electronic and magnetic properties of the fully or partially hydrogenated BNNRs and will lead to better usage of these materials in the future design of functional nanodevices. Note that the wide-band gap of BN nanomaterials is a serious obstacle for their application in electronics, despite their high thermal and chemical stabilities. On the basis of these density functional theory (DFT) computations, we proposed a simple and effective approach to modulate the band gap of zBNNRs by changing the hydrogenation coverage and to realize a semiconductor→half-metal→metal transition accompanied by a nonmagnetic→magnetic transfer. Consequently, it is highly feasible that these intriguing properties can be fabricated in the unitary BN-based nanomaterials, which is advantageous for the design of automatic integration.

2. Computational Method

The generalized gradient approximation (GGA) with the PW91 functional[72] and a 400-eV cutoff for the plane-wave basis set were employed for all the DFT computations with the Vienna ab initio simulation package (VASP).[73−76] The projector-augmented plane wave (PAW)[77,78] was used to model the electron−ion interactions. Interactions between two ribbons and their images were avoided in our computational supercell models, for which the distance between two ribbons is longer than 10 Å in both zigzag and armchair hydrogenated BNNRs. Five k points were used for sampling the 1-D Brillouin zone, and the convergence threshold was set as 10^{-4} eV in energy and 10^{-3} eV/Å in force. The positions of all the atoms in the supercell were fully relaxed during the geometry optimizations. On the basis of the equilibrium structures, 21 k points were used to compute band structures.

The formation energies of fully hydrogenated BNNRs with various widths are estimated by the definition as $E_f = E_{BNH} - \chi_B\mu_B - \chi_N\mu_N - \chi_H\mu_H$ to determine the relative stabilities of these hydrogenated nanoribbons, in which E_{BNH} is the cohesive energy per atom of fully hydrogenated BNNRs, χ_i (i = B, N, and H, respectively) is the mole fraction of the i atom in the nanoribbon, μ_H is the binding energy per atom of the H_2 molecule, and μ_B and μ_N are the cohesive energies per B atom and N atom in infinite pristine BN single layer, respectively. This approach has been employed widely to investigate the relative stability of some nanostructures based on GNRs.[22,29,39] Moreover, the binding energy per hydrogen atom of the hydrogenated BNNRs and BN sheet is computed by the definition as $E_b = (nE_H + E_{BN} - E_{H\text{-}BN})/n$, where n is the number of H atoms, and E_H, E_{BN}, and $E_{H\text{-}BN}$ are the energies of H atom, bare BNNRs/BN sheet, and corresponding hydrogenated structures, respectively.

3. Results and Discussion

3.1. 2D Infinite Fully Hydrogenated BN Single Layer. First, the 2D infinite fully hydrogenated BN single layer was investigated in a 6 × 6 supercell, which is composed of 36 B, 36 N, and 72 H atoms. Similar to 2D carbon graphane,[10,39] the most stable form prefers a regular chairlike structure with hydrogen atoms linked to B atoms on one side and those linked to N atoms on the other side (Figure 1a), like the case of perhydrogenated BN nanotubes.[79] All of the angles between B or N atoms and their conjoint four atoms (three N or B atoms and one H atom) are about 109°, suggesting that the B and N atoms in the fully hydrogenated BN single layer are typical sp^3 hybridization. Consequently, the B−N bonds length in the fully hydrogenated BN single layer are in the range of 1.566−1.581 Å, which is close to the B−N single bond, but much longer than that (1.445−1.447 Å) in the BN single layer with sp^2 hybridization. The B−H and N−H bond lengths in the fully

(72) Perdew, J. P.; Chevary, J. A.; Vosko, S. H.; Jackson, K. A.; Pederson, M. R.; Singh, D. J.; Fiolhais, C. *Phys. Rev. B* **1992**, *46*, 6671–6687.
(73) Kresse, G.; Hafner, J. *Phys. Rev. B* **1993**, *47*, 558–561.
(74) Kresse, G.; Hafner, J. *Phys. Rev. B* **1994**, *49*, 14251–14269.
(75) Kresse, G.; Furthmuller, J. *Comput. Mater. Sci.* **1996**, *6*, 15–50.
(76) Kresse, G.; Furthmuller, J. *Phys. Rev. B* **1996**, *54*, 11169–11186.
(77) Blochl, P. E. *Phys. Rev. B* **1994**, *50*, 17953–17979.
(78) Kresse, G.; Joubert, D. *Phys. Rev. B* **1999**, *59*, 1758–1775.
(79) Tanskanen, J. T.; Linnolahti, M.; Karttunen, A. J.; Pakkanen, T. A. *J. Phys. Chem. C* **2008**, *112*, 2418–2422.

Table 1. Energy Difference (ΔE) between Spin-Polarized and Spin-Unpolarized States and Total Magnetic Moments (M) per Unit Cell for fH-N_z-zBNNRs with Various Widths ($N_z = 6-11$)

N_z	ΔE (meV)	M (μ_B)
6	−20.6	0.496
7	−29.9	0.601
8	−37.8	0.684
9	−43.0	0.717
10	−46.9	0.755
11	−48.0	0.766

hydrogenated BN single layer are 1.198 and 1.036 Å, respectively. Moreover, our DFT computation shows that the 2D fully hydrogenated BN single layer is a nonmagnetic semiconductor with a direct band gap of 3.05 eV.

3.2. Geometries of 1D Fully Hydrogenated BNNRs. Similar to BNNRs, two types of fully hydrogenated BNNRs with zigzag or armchair edges were considered in this work. Following the convention of the BNNRs, as shown in Figure 1b, the structures of zigzag and armchair fully hydrogenated BNNRs are also classified by the number of zigzag chains N_z and dimer lines N_a across the ribbon width, respectively. In this study, the fully hydrogenated zigzag and armchair BNNRs are named as fH-N_z-zBNNR and fH-N_a-aBNNR, respectively.

A series of fH-N_z-zBNNRs and fH-N_a-aBNNRs with various widths (N_z = 6, 7, 8, 9, 10, 11 and N_a = 7, 9, 11, 13, 15, 17, 19) were computed. In both fH-N_z-zBNNRs and fH-N_a-aBNNRs, all of the inner B−N, B−H, and N−H bonds are almost the same as the corresponding values in the 2D fully hydrogenated BN sheet, and the sp^3 hybridization is kept. The edge B and N atoms are linked to two hydrogen atoms to remove the dangling bonds. These edge B−H bonds (1.224−1.235 Å for zigzag ribbons, and 1.208−1.224 Å for armchair ribbons) are longer than the inner B−H bonds (1.198−1.201 Å), while the edge N−H bonds (1.028−1.037 Å for zigzag ribbons, and 1.026−1.028 Å for armchair ribbons) are slightly shorter or longer than the inner N−H bonds (1.035−1.036 Å).

3.3. Electronic and Magnetic Properties of 1D Fully Hydrogenated BNNRs. Both spin-polarized and spin-unpolarized computations were performed to determine the ground state of fH-zBNNRs and fH-aBNNRs. Our DFT computations show that fH-aBNNRs are nonmagnetic semiconductors, the same as the analogous armchair graphane nanoribbons.[39] The detailed discussion on electronic and magnetic properties of fH-aBNNRs is given in Section I of the Supporting Information.

However, different from the carbon counterparts, the fH-zBNNRs are magnetic, as revealed by the lower total energy by the spin-polarized computation. Table 1 summarizes the energy difference (ΔE) between the ferromagnetic and nonmagnetic states and total magnetic moments (M) per unit cell of a series of fH-N_z-zBNNRs ($N_z = 6-11$). The ΔE and M values increase with increasing the ribbon width. The fH-6-zBNNR has the lowest ΔE (20.6 meV) and M (0.496 μ_B), while the fH-11-zBNNR has the highest ΔE (48.0 meV) and M (0.766 μ_B). Moreover, to confirm the ground state (ferromagnetic state) of the fH-zBNNRs, three antiferromagnetic configurations of fH-8-zBNNR were investigated (Figure S2 and Table S1). Our computational results show that these three antiferromagnetic configurations are energetically less favorable than the ferromagnetic one, by 5.8, 37.6, and 36.7 meV, respectively (Table S1). Clearly, the ferromagnetic configuration is the ground state of the fH-zBNNRs.

To obtain further insight into the magnetism of fH-zBNNRs, we computed the spin density distribution of fH-8-zBNNR (Figure 2a), which reveals that unpaired spin mainly concentrates on the edge B and two related H atoms. The unsaturated B edge atoms should be responsible for the magnetic behavior of fH-zBNNRs.

To understand the reason for the unsaturation of the edge B atoms, we initially show the bonding mode of theoretically studied two-hydrogen-terminated 6-zigzag GNR,[20] where the single−double bond alternation is found for inner C atoms with sp^2 hybridization, and the π bonds are perpendicular to the periodic direction (Figure 2b). As the analogue, the two-hydrogen-terminated 8-zigzag BNNR has similar bonding manner (Figure 2b), where the inner B and N atoms also adopt typical sp^2 hybridization, and the remaining vacant p orbital of each inner B atom receives lone pair electrons of its neighboring N atom to form a π bond between B and N atoms perpendicular to the periodic direction. As a result, no N atom donates its electron to the edge B atoms in the two-hydrogen-terminated zigzag BNNRs, which results in unsaturation of the edge B atoms.

The fH-zBNNRs can be considered as a product of further hydrogenation of two-hydrogen-terminated zigzag BNNRs, in which each B═N double bond is saturated by two H atoms at the opposite sides of ribbons, and each inner B/N atom adopts typical sp^3 hybridization, and is saturated to satisfy the octet rule, while the unsaturation of edge B atoms is kept, and the bond between each edge B and two related H atoms can be described by two resonant structures containing one two-electron and one single-electron B−H bonds (Figure S3). Because of the larger electronegativity of H than B atoms, unpaired spin density is mainly distributed on the related H atoms instead of the edge B atoms (Figure 2a). The unsaturation of the B edge atoms can also be reflected by the much longer edge B−H bond length (1.224−1.235 Å) than those (1.198−1.201 Å) of inner B−H bonds.

The edge unsaturated B-2H states of fH-zBNNRs result in not only the different magnetic but also the different electronic behaviors between fH-zBNNRs and fH-aBNNRs. In contrast to the fH-aBNNRs, the fH-zBNNRs exhibit typical metallic behavior independent of ribbon width. As illustrated in Figure 2c, one energy level in each spin channel crosses the Fermi level in fH-8-zBNNR. Note that two-hydrogen-terminated zigzag BNNRs[59] are also metallic, while zBNNRs[54] and zigzag graphane nanoribbons[39] are wide-band gap semiconductors. To understand the origin of the metallic band structure, we plotted the total density of states (TDOS) and local density of states (LDOS) of fH-8-zBNNR (Figure 2d). Clearly the state crossing the Fermi level in spin-down channels is dominated with the 2p electrons of edge N atoms, while the state crossing the Fermi level in the spin-up channel is from the 2p electrons of edge B atoms and the s electrons of H atoms linked to the edge B atoms.

3.4. Stabilities of 1D Fully Hydrogenated BNNRs. The relative stability of nanostructures is important to evaluate the possibility of experimental realizations. Here, the formation energies as a function of the ribbon width are computed for fH-zBNNRs and fH-aBNNRs (Figure 3). The formation energy of fH-zBNNRs increases monotonically with increasing ribbon width, while that of fH-aBNNRs displays the opposite trend, which is mainly attributed to the different stabilities of zigzag and armchair edges for pristine BNNRs: armchair edge exhibits higher stability than the zigzag one. Similar to graphane nanoribbons,[39] the negative formation energies suggest that the formation of both types of fH-BNNRs is favorable energetically

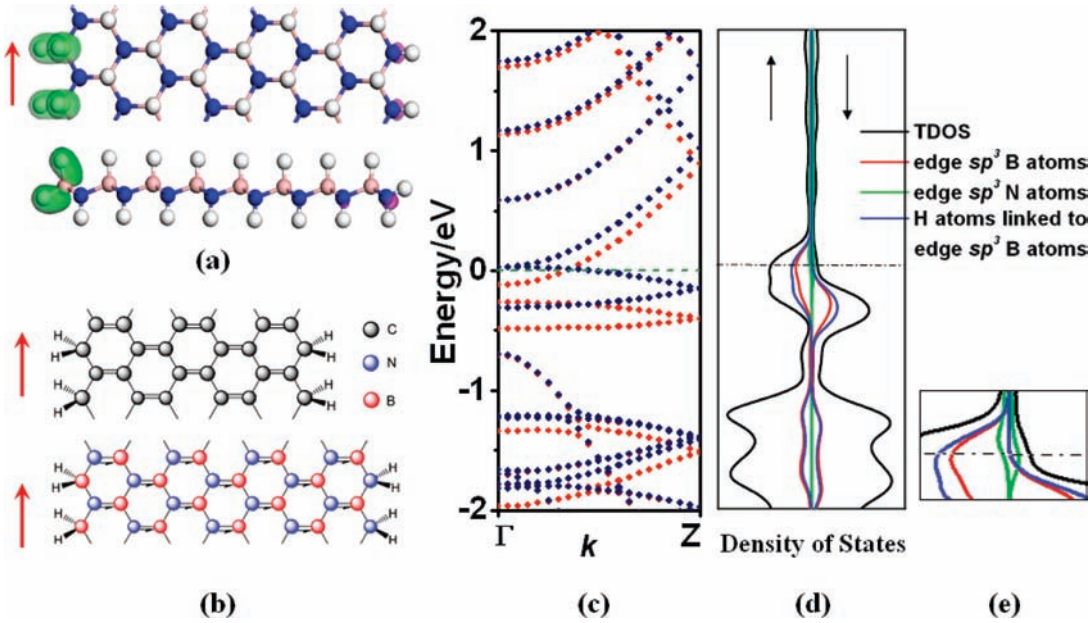

Figure 2. (a) Top and side views of spatial spin distribution (the red arrow represents the periodic direction of the ribbon). (b) The bonding modes of 6-zigzag GNR (upper) and 8-zigzag BNNR (below) terminated by two hydrogen atoms. (c) The band structure (the Fermi level is set to zero; the spin-up (↑) and spin-down (↓) electrons are denoted by blue and red dot lines, respectively), and (d) TDOS and LDOS of *f*H-8-zBNNR. (e) The zoom on the region about the Fermi level in (d).

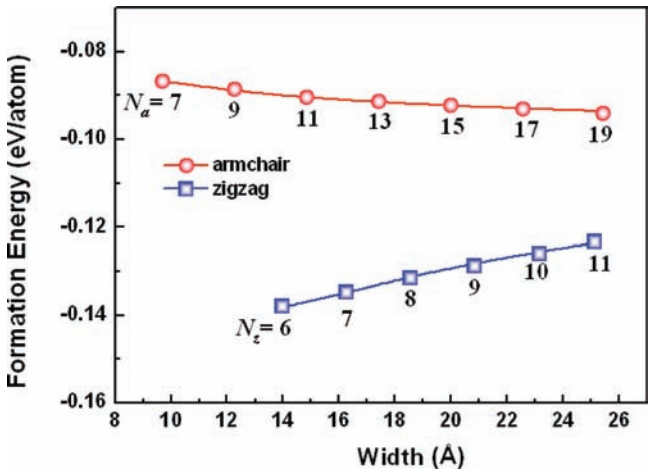

Figure 3. The formation energy of *f*H-N_z-zBNNRs ($N_z = 6-11$) and *f*H-N_a-aBNNRs ($N_a = 7-19$) as a function of the ribbon width.

by hydrogenating the corresponding BNNRs, which indicates a potential experimental route to transform BNNRs to *f*H-BNNRs.

To examine the stabilities of hydrogenated BN sheet/ribbons, we computed the binding energies of hydrogen atoms on 2D BN single-layer, *f*H-8-zBNNR and *f*H-11-aBNNR, which are 2.074, 2.364, and 2.363 eV, respectively. Obviously, these binding energies are large enough to prevent the disassociation of the bound H atoms from the surface of hydrogenated BNNRs/BN sheet at the general operational conditions.

3.5. Electronic and Magnetic Properties of Partially Hydrogenated Zigzag BN Nanoribbons. Numerous efforts were devoted to modulate the wide-band gap of BNNRs,[53,58−61] because the wide-band gap of BN nanomaterials is a substantial obstacle for their applications in electronics. For example, by applying an external transversal electric field, the band gap of bare zBNNRs can undergo metallic−semiconducting−half-metallic transition.[46] By means of different edge modifications and the formation of SW defects, the band gap of the BNNRs can be altered, and the corresponding decorated BNNRs present semiconducting,[58,62] metallic,[59] or half-metallic[60,61] behaviors. Here, we provide a simple way by changing the hydrogenation coverage of zBNNRs to modulate the wide-band gap more effectively, and to realize the different electronic and magnetic properties in the same BN-based nanomaterial, which is advantageous for the design of automatic integration.[37,80] It is a great dream that scientists continuously pursue to fabricate the diverse electronic and magnetic properties in unitary material background.

As mentioned above, by fully hydrogenating zBNNRs, their electronic and magnetic properties can be transformed from nonmagnetic semiconductors to magnetic metals, and the corresponding band gap is effectively reduced from the original value (about 4.00 eV)[54] to zero. The dramatic changes of electronic and magnetic properties inspired us to further investigate the partially hydrogenated zBNNRs, which are constructed by the combination of BNNRs and *f*H-BNNRs as building blocks. Note that, for the partially hydrogenated zBNNRs with the same hydrogenation coverage, the formation of this configuration consisting of the blocks is more favorable energetically than the structures with H-atom arbitrary distribution, as revealed by our computational results in Section IV of Supporting Information. Thus, the partially hydrogenated BNNRs constructed by BNNR and *f*H-BNNR blocks are only considered in this work. It is expected that a multiplex transformation of electronic and magnetic properties in this kind of the partially hydrogenated zBNNRs can be obtained with different hydrogenation degrees. Our approach is also motivated by Singh et al.'s interesting theoretical finding that the transition from small-band-gap semiconductors to metals occurs for the zigzag graphene "nanoroad" (the partially hydrogenated graphene),[37] and by Wu et al.'s theoretical prediction that zigzag

(80) Li, J.; Zhou, G.; Chen, Y.; Gu, B.; Duan, W. *J. Am. Chem. Soc.* **2009**, *131*, 1796–1801.

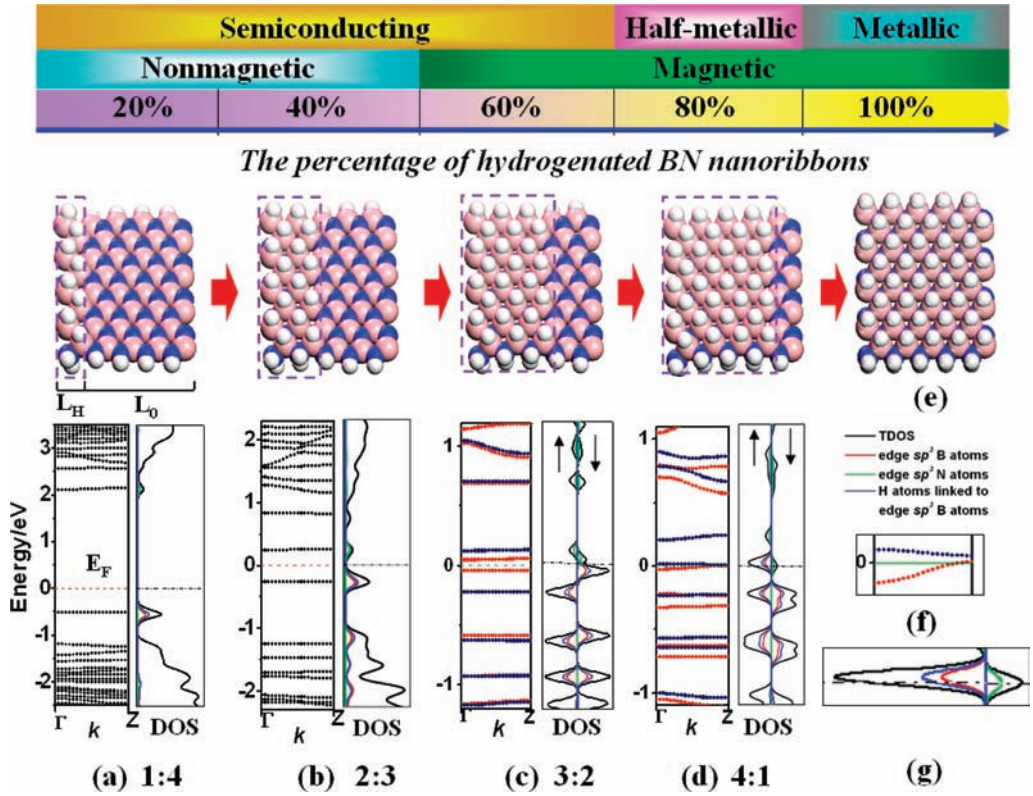

Figure 4. Structural and electronic properties of the *p*H-8-zBNNRs with the different ratios of L_H to L_0: (a) 1:4, (b) 2:3, (c) 3:2, and (d) 4:1. One unit corresponds to the part in the dash lines in (a), and the L_H and L_0 are respective unit numbers of hydrogenated and pristine BNNR blocks. The blue and red dot lines denote the spin-up (↑) and spin-down (↓) channels, respectively, for the band structures of (c) and (d). (e) The structure of *f*H-zBNNR. Parts f and g show the zooms on the region about the Fermi level of band structure and DOS of (d).

GNRs and graphene decorated by OH/H and F groups can be changed to half-metals provided that the width of the undecorated carbon part is wide enough, and the electronic behavior of the decorated graphene is very similar to that of edge decorated zigzag GNRs.[30]

Several partially hydrogenated 8-zBNNRs with different hydrogenation ratios of L_H to L_0 (1:4, 2:3, 3:2, and 4:1) were investigated. The partially hydrogenated zigzag BNNRs with different ratios are represented as *p*H-zBNNRs (L_H:L_0), in which L_H and L_0 are the respective unit numbers of the hydrogenated and pristine BNNR blocks along the periodic direction of BN ribbon, where one unit corresponds to the part in the dash lines in Figure 4a. The fully relaxed structures and corresponding band structures are presented in Figure 4, for which a supercell including 40 B and 40 N atoms was employed in our computations. As expected, appealing and diverse transformations in electronic and magnetic properties occur with increasing the hydrogenation percentage in zBNNRs.

The *p*H-zBNNR (1:4) is a nonmagnetic semiconductor; although significantly reduced as compared to the pristine BNNR (ca. 4.00 eV),[54] its band gap is still rather wide (2.62 eV, Figure 4a). Increasing the hydrogenation ratio to 2:3 further decreases the band gap (0.50 eV, Figure 4b), and the according nanostructure is still a nonmagnetic semiconductor. When the hydrogenation ratio is increased to 3:2, the hydrogenated BNNR becomes a magnetic semiconductor, for which the band gaps of the spin-up and spin-down channels are 0.35 and 0.09 eV, respectively (Figure 4c). The corresponding DOS results (Figure 4a−c) reveal that their highest-energy valence bands originate from the 2p electrons of edge B atoms with sp^3 hybridization and s electrons of the H atoms linked to these edge B atoms, and their lowest-energy conduction bands are mainly from the 2p electrons of edge N atoms with sp^3 hybridization.

When the hydrogenation ratio reaches 4:1, the typical half-metallic behavior is observed, for which one level in the spin-down channel crosses the Fermi level and the corresponding level in the spin-up channel does not, although this level is very close to the Fermi level (Figure 4d). The computed DOS (Figure 4d) shows that the state crossing the Fermi level is dominated with the 2p electrons of edge N atoms with sp^3 hybridization, while the state quite near the Fermi level is from the 2p electrons of edge B atoms with sp^3 hybridization and s electrons of the H atoms linked to these B atoms. Finally, by fully hydrogenating zBNNRs, these ribbons are drastically converted to magnetic metals for both spin-up and spin-down channels, as discussed above.

Comparing the computed DOS graphs (Figures 4a−d, 2d, and S5c) reveals that, for all of the hydrogenated zBNNRs, their bands around the Fermi level are dominated by edge B/N atoms with sp^3 hybridization and the related H atoms, and increasing the hydrogenation percentage causes both highest-energy valence and lowest-energy conduction bands shift toward the Fermi level until crossing it, which results in the significant decease of band gap of these hydrogenated BNNRs along with increasing hydrogenation ratio.

Clearly, changing the hydrogenation percentage can effectively modulate the band gap of zBNNRs, and correspondingly causes the considerably diverse transformations of the electronic and magnetic properties: a semiconductor→half-metal→metal transition, accompanied by a nonmagnetic→magnetic transfer with increasing hydrogenation coverage. Note that the half-metallicity of *p*H-zBNNR (4:1) is not robust; however,

the half-metallic behavior can be sustained for partially hydrogenated zBNNRs with a slightly smaller hydrogenation ratio such as *p*H-zBNNR (3:1), which exhibits more robust half-metallicity than *p*H-zBNNR (4:1), as revealed by our computational results (Figure S5).

Moreover, to reveal the stabilities of *p*H-BNNRs, we computed the binding energies of hydrogen atoms on *p*H-8-zBNNRs with the ratios of 1:4, 2:3, 3:2, and 4:1, which are 3.057, 2.670, 2.492 and 2.393 eV, respectively. Clearly, such large binding energies can effectively inhibit the disassociation/diffusion of the bound H atoms on the surface of the *p*H-BNNRs.

4. Conclusion

The electronic and magnetic properties of fully and partially hydrogenated BNNRs were investigated by means of DFT computations. In contrast to the analogous graphane nanoribbons, which are nonmagnetic semiconductors, the *f*H-aBNNRs are nonmagnetic wide-band gap semiconductors, while the zigzag counterparts are magnetic and metallic, independent of ribbon widths. Both *f*H-aBNNRs and *f*H-zBNNRs have favorable formation energies, indicating a great possibility of realizing them by hydrogenating the corresponding BNNRs in future experiments.

Zigzag BNNRs and *f*H-zBNNRs are used as building blocks to construct the partially hydrogenated zBNNRs, and the following intriguing properties are revealed: (1) When the hydrogenated BNNR block is minor in the whole ribbon, the *p*H-BNNRs are nonmagnetic semiconductors, and their band gaps decrease significantly with increasing the hydrogenation coverage. (2) When the hydrogenated BNNR block is dominant, the *p*H-BNNRs present manifold transition, that is, semiconductor→half-metal→metal transition accompanied by nonmagnetic→magnetic transfer with increasing the ratio of L_H to L_0. Obviously, the percentage of hydrogenation can effectively control the band gap of zBNNRs and plays a crucial role of engineering the electronic and magnetic properties of zBNNRs. Although the half-metallicity is not robust, this behavior is sustained for *p*H-zBNNRs.

Our computations give us a valuable experimental implication: intriguing electronic and magnetic properties of hydrogenated zigzag BNNRs can be precisely and effectively engineered by tuning an optional hydrogenation ratio in future experiments. It is very promising that the semiconducting, half-metallic, metallic, nonmagnetic, as well as magnetic hydrogenated BNNRs can be patterned on the unitary BN-based nanomaterial in view of the automatic integration. We are highly expecting the experimental realization of these functions in the BN-based nanodevices.

Acknowledgment. This work was supported in the U.S. by NSF Grant CHE-0716718, the Institute for Functional Nanomaterials (NSF Grant 0701525), the U.S. Environmental Protection Agency (EPA Grant No. RD-83385601), and in part by the National Science Foundation through TeraGrid resources, and in China by NSFC (20873067) and NCET. G. T. Yu thanks the start-up fund (450080011085) from Jilin University. The authors thank the Computational Center for Nanotechnology Innovations (CCNI) at Rensselaer Polytechnic Institute for the use of the supercomputer facilities. This paper is dedicated to Professor Paul von Ragué Schleyer on the occasion of his 80th birthday.

Supporting Information Available: (I) Electronic and magnetic properties of 1D *f*H-aBNNRs (Figure S1); (II) the antiferromagnetic states of *f*H-zBNNR (Table S1 and Figure S2); (III) resonance structure between edge B and two related H atoms of *f*H-zBNNR (Figure S3); (IV) structures of *p*H-BNNRs with arbitrary distribution of hydrogen atoms (Table S2 and Figure S4); and (V) the electronic property of *p*H-zBNNR (3:1) (Figure S5). This material is available free of charge via the Internet at http://pubs.acs.org.

JA908475V